

StringTouch: A Non-occlusive 3DoF Haptic Interface using String Structures for Modulating Finger Sensations

YoungIn Kim

HCI Lab

School of Computing, KAIST
Daejeon, Republic of Korea
youngin@kaist.ac.kr

Jisu Yim

HCI Lab

School of Computing, KAIST
Daejeon, Republic of Korea
yimjisu99@kaist.ac.kr

Yohan Yun

HCI Lab

School of Computing, KAIST
Daejeon, Republic of Korea
yohanme@kaist.ac.kr

Donghyeon Ko*

HCI Lab

School of Computing, KAIST
Daejeon, Republic of Korea
dong7863@gmail.com

Geehyuk Lee

HCI Lab

School of Computing, KAIST
Daejeon, Republic of Korea
geehyuk@gmail.com

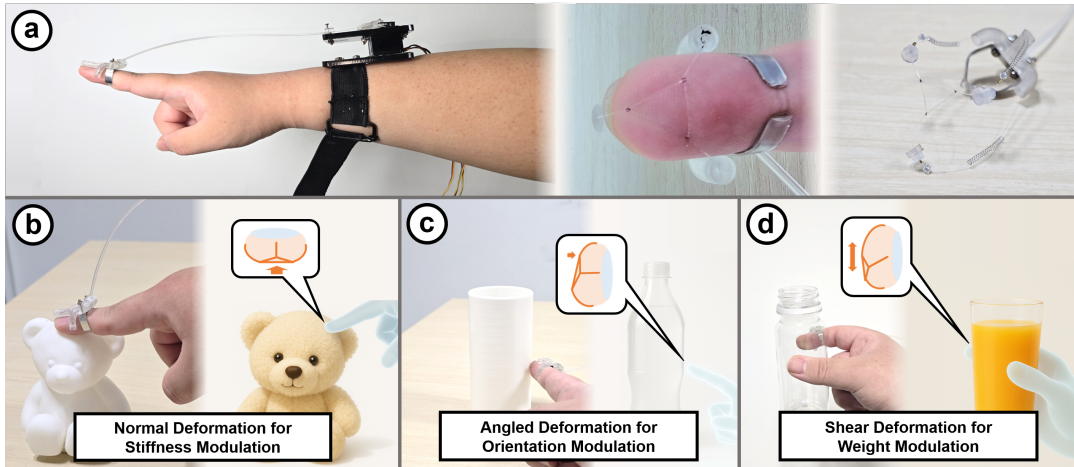


Figure 1: (a) We developed StringTouch, a haptic device that modulates the perception of a proxy's physical properties. A unique feature of our device is its 3DoF mechanism that pulls nylon strings from three directions without occluding the fingertip, enabling the rendering of (b) stiffness, (c) orientation, and (d) weight perception.

Abstract

Providing realistic and diverse tactile feedback during interactions with objects in virtual and augmented reality, various studies have explored the use of tangible proxies. However, tangible proxies face limitations due to their fixed physical properties, restricting the expression of various stiffness, weights, and shapes. To address these issues, we propose StringTouch, a device modulating sensations from proxies without obstructing the fingers to preserve finger sensitivity. StringTouch modulates sensations utilizing 0.2mm thin nylon threads to deform fingers with 3DoF. In a user study (n

= 12), our string structure showed better performance in distinguishing orientation, roughness, and weight than conditions using a 0.1 mm latex finger cot and was comparable to bare fingers in some of the discriminating tasks. Another experiment (n = 12) verified the device's capability to modulate orientation, stiffness, and weight perceptions. Finally, in a user study (n = 10) in proxy-based VR scenarios (pouring water, touching a teddy bear, touching a bottle), participants preferred StringTouch over bare finger interactions, with most of them reporting enhanced presence.

CCS Concepts

• Human-centered computing → Haptic devices

Keywords

Haptic Device, Wearable Device, Extended Reality, Virtual Reality

ACM Reference Format:

YoungIn Kim, Jisu Yim, Yohan Yun, Donghyeon Ko, and Geehyuk Lee. 2025. StringTouch: A Non-occlusive 3DoF Haptic Interface using String Structures

*Donghyeon Ko is currently at UHCI Lab, University of Ulsan, Republic of Korea.



This work is licensed under a Creative Commons Attribution 4.0 International License.
UIST '25, Busan, Republic of Korea

© 2025 Copyright held by the owner/author(s).
ACM ISBN 979-8-4007-2037-6/2025/09
<https://doi.org/10.1145/3746059.3747658>

for Modulating Finger Sensations. In *The 38th Annual ACM Symposium on User Interface Software and Technology (UIST '25), September 28–October 1, 2025, Busan, Republic of Korea*. ACM, New York, NY, USA, 14 pages. <https://doi.org/10.1145/3746059.3747658>

1 Introduction

Despite recent advances in virtual reality (VR) and augmented reality (AR) technologies, delivering realistic tactile feedback remains challenging. While diverse, active wearable haptic devices have been introduced [2, 6, 17, 21], they are often vibrotactile or force-feedback systems and fall short of simultaneously and precisely providing haptic cues for nuanced physical attributes, such as shape, weight, and stiffness, despite complex structures [8, 34, 58]. For example, using wearable devices to provide effective haptic cues for a glass cup's contours, weight, and textures remains difficult.

In contrast, tangible proxies effectively convey nuanced properties such as weight, shape, and material properties [8, 12, 19]. Physical props matching virtual objects' geometry, texture, and weight offer high haptic realism and visual-haptic coherence, enhancing immersion and presence [12, 19, 22]. However, the fixed physical properties of proxies limit flexibility across varied virtual contexts or dynamic scenarios [8, 13]. For example, a glass proxy cannot replicate the softness of silicone nor the changing weight of a filling virtual cup. This challenge is being addressed by recent research with shape-changing proxies regarding object forms [16] or weight [57] but is yet to be explored for other object properties, such as roughness, hardness, and curvature.

Recent research noted the complementary strengths of wearable haptic devices and tangible proxies and investigated the opportunities for non-obstructive wearable haptic interfaces combined with tangible proxies, aiming to overcome the limited expressive capability of static tangible proxies. Early studies include nail-mounted vibration or mechanical actuators [25, 44] and proximal (off the fingertip) finger-worn skin deformation devices [10, 39, 45]. They explored the possibility of conveying substituted tactile feedback to the fingertip without occluding it. These devices were shown to modulate stiffness, weight, or elasticity perceptually. Nevertheless, existing methods, limited mainly to vibration or basic skin compression, inherently restrict the range of tactile cues achievable. For example, hRing [39] and Tinguy's approach [10] effectively simulate consistent pressure or gentle shear sensation but fall short of expressing nuanced attributes such as curvature or dynamic weight changes. In a more recent study, thin-electrode-embedded tattoo films with small holes delivered basic tactile sensations while minimally obstructing natural touch sense [51]. The study showed that creating a non-occlusive space by punching small holes in tattoo paper could improve finger sensitivity while providing a similar level of tactile feedback. However, the electrode stimulation was limited to pressure and vibration cues.

To overcome these limitations and expand the tactile rendering capability of a single proxy, we designed **StringTouch**, a non-occluding, 3-DoF fingertip haptic device employing a thin nylon string structure. StringTouch deforms the fingertip from three distinct directions, modulating tactile perceptions, such as weight, stiffness, and orientation while maintaining tactile sensitivity close to that of the bare fingertip for discrimination of orientation, stiffness, roughness, and weight. With StringTouch, we aim to change

users' haptic perception of tangible proxies, e.g., light-weight proxies as heavier or rigid proxies as softer, thereby expanding the expressive power of tangible proxies. For this goal, StringTouch should not block the fingertip's natural tactile sensation and should be able to deliver required tactile cues to the fingertip at the same time. Therefore, we have three research questions:

- **RQ1:** Does the non-occlusive tactic design of StringTouch preserve the fingertip's natural tactile sensation?
- **RQ2:** Can StringTouch provide required tactile cues to the fingertip for diverse object properties, such as weight, stiffness, planar orientation?
- **RQ3:** Can StringTouch modulate the fingertip's tactile perception while users are interacting with tangible objects?

To investigate these questions, we conducted three experiments described in Sections 4, 5, and 6. In Section 4, twelve participants compared tactile stimuli—orientation, stiffness, roughness, and weight—under four conditions (bare finger, Y-shaped string, triangular string, and a thin latex finger cot), revealing that the triangular string preserved tactile sensitivity similarly to the bare finger, while the cot notably degraded performance. Section 5 used normal, shear, and angular skin deformations at different intensities to adjust perceived weight, stiffness, and orientation, showing that twelve participants experienced gradual increases in perceived weight, stiffness, and angular cues. Section 6 involved ten participants in VR scenarios (pouring water, touching a teddy bear, and stroking curved surfaces) with and without StringTouch feedback, resulting in significantly higher realism and preference ratings for the StringTouch. The contributions of this study are two-fold:

- The **StringTouch**, a non-occlusive 3DoF haptic device enabling 3DoF finger skin deformations.
- Empirical validation of StringTouch's applicability in proxy-based interaction, leveraging its non-occlusive design and tactile modulation capabilities

2 Related Works

2.1 Proxies for Tactile Realism and Interaction Consistency

Typical vibrotactile or force-feedback devices struggle to simultaneously and finely render tactile sensations such as shape, weight, or stiffness, and often entail complex implementations [8, 34, 54, 58]. As an alternative, tangible proxies—physical objects to interact with virtual counterparts—can effectively convey intricate physical properties [12, 19]. Such proxies deliver authentic geometry and material cues, greatly enhancing tactile realism and visual-haptic consistency, thus anchoring user perception and increasing immersion [20, 22, 46].

However, fixed physical attributes (e.g., shape, weight, texture, stiffness) of traditional proxies limit their adaptability in diverse or dynamic contexts [27]. While prior studies attempt to mitigate shape [5, 19, 24], travel distance [13], and weight [11] mismatches using multiple props or visual-haptic illusions [1], these solutions remain insufficient in fully bridging the proxy–virtual object gap [1, 14, 33]. Recent approaches employing dynamic proxies (e.g., internal weight shifting [57] or shape deformation [16]) improved realism by adaptively matching virtual content. Still, dynamically

changing surface roughness, hardness, or macroscopic form remains challenging, often necessitating multiple proxies. Replicating complex structures of dynamic proxies for various materials and forms is inherently limited. Alternatively, directly modulating fingertip sensations—rather than proxy characteristics—may provide a simpler, versatile solution. Our research addresses these challenges with a non-occlusive wearable device that dynamically alters perceived proxy attributes such as weight, stiffness, and orientation.

2.2 Tactile Perception and Finger Freedom

Tactile perception strongly depends on finger freedom during object exploration, activating diverse tactile receptors via natural interactions (e.g., pressing, grasping, stroking) [15, 29]. Restricting finger movement or occluding skin contact significantly reduces tactile sensitivity and dexterity [30]. Previous studies have demonstrated that masked fingers due to gloves or bulky haptic devices impair sensitivity [4, 31, 56] and dexterity [56]. Even thin coverings like tattoo paper may alter contact mechanics and degrade tactile performance [3, 51, 55]. Nittala et al. showed that even films of 2.5 um can significantly reduce the discrimination sensitivity of textured surfaces depending on rigidity [35]. The attenuation of tactile sensation is also prominent in situations requiring delicate object exploration or tool use, where users perform better when their fingertips are unencumbered and can directly feel the target object [51, 56]. Due to these issues, minimal occlusion is critical in haptic proxy design for VR/AR, ensuring that users can naturally touch and manipulate objects [40, 43]. Our approach aligns with this principle by employing an open, thin-string tactors that maintains fingertip exposure for direct tactile exploration.

2.3 Less-occlusive Tactile Feedback Techniques for Modulating Sensations

Given the importance of fingertip freedom, researchers have explored minimally occlusive tactile feedback methods.

A representative approach involves the use of thin tattoo paper. As discussed in Section 2.2, this may introduce some degree of tactile masking; however, it reflects an effort to deliver tactile feedback while keeping fingertip sensitivity. Ultra-thin electrode tattoo films can deliver subtle tactile sensations with minimal obstruction [37, 49, 51, 55] but these films encounter issues such as unintended electrode-skin interactions [37, 49] or fragility [35].

Another strategy involves attaching haptic actuators to fingernails or the back of the hand, freeing the fingerpad. Devices like Haplets use nail-mounted vibration modules to simulate transient events and textures [44]. Maeda et al. [25] combined rollers with fingernail vibration actuators, offering richer tactile cues but remaining limited in representing continuous, three-dimensional deformations such as changing weight or curvature.

Alternative methods have employed proximal finger-mounted actuators to deform skin and simulate sensations without covering the fingertip. Examples include hRing, which generates normal and shear forces via a ring-like device positioned around the proximal phalanx [39, 45], and Tinguy's belt-type device that adjusts perceived stiffness by lateral skin deformation [10]. These approaches simulate pressure or frictional cues but face difficulty simultaneously rendering complex tactile attributes like curvature or dynamic

weight changes. Additionally, placing actuators directly on fingers can introduce unwanted physical weight and inertia.

Recently, thin string-based devices have recently emerged to virtual grip forces with minimal occlusion, like object-picking tasks in VR [56]. This system enhances precision and execution time with higher usability than gloves in tasks like object manipulation. Nevertheless, their device offers simple pulling forces rather than nuanced sensory modulation. Distinct from prior works, our approach employs a 3DoF actuation mechanism to deform the fingerpad skin in various ways, dynamically altering tactile perceptions—such as weight, hardness, or curvature—mimicking virtual objects while preserving fingertip openness and natural exploration.

3 Implementing StringTouch

StringTouch is a wearable haptic device, with the frame worn on the finger and the actuator secured to the wrist via an elastic band (Figure 1(a)). Its implementation requires appropriate string thickness, structure, size, and suitable actuation components. The following sections describe these design elements in detail.

3.1 Fabricating the String Structure

3.1.1 String material and thickness. We selected a nylon fishing line (YUGUIFEI DPLS) for its optimal balance between thinness, durability, and elasticity. The string's width must allow the finger exposed between the structures to naturally touch objects while avoiding pain due to increased pressure from a thin width. A preliminary in-lab pilot ($n = 5$) indicated that strings thicker than 0.3 mm noticeably occluded tactile sensation, while those thinner than 0.1 mm caused discomfort or slight pain under tension. In addition, due to the 0.1 mm-tactor fabricated to the shape described in Section 3.1.2 being considered to have potential durability concerns, we chose a 0.2 mm thickness. The 0.2 mm nylon string can support maximum 5 kg of load.

3.1.2 Structure shape. To achieve 3DoF deformation, we explored two configurations: a Y-shape, where three strings converge at a single central point, and a triangular shape, with strings connecting three vertices, leaving a central opening for direct fingertip contact. These structures were fabricated using a 0.2 mm nylon fishing line with an ultrasonic welder, keeping the thickness of vertices also to 0.2 mm. We experimentally compared sensory occlusion between these shapes in Section 4 and chose the better one.

3.1.3 Structure size. While the Y-shaped structure is uniform across finger sizes, the triangular configuration depends on finger width. Given typical index finger widths ranging from 15–20 mm [9, 23], we fabricated triangles with side lengths of 8 mm, 10 mm, and 12 mm to accommodate finger widths of 12–21 mm (finger width 12mm–14mm: 8, 14mm–17mm: 10, 17mm–21mm: 12). Participants were recruited without size restrictions, but no finger widths fell outside this range. The fabricated tactor was designed to be mounted on the terminal flat surface of the index finger's distal phalanx.

3.2 Mechanical Structure

The structure of StringTouch comprises three primary components: a frame that securely mounts on the finger and supports the tactor, a Bowden cable to transmit tension from remotely located motors

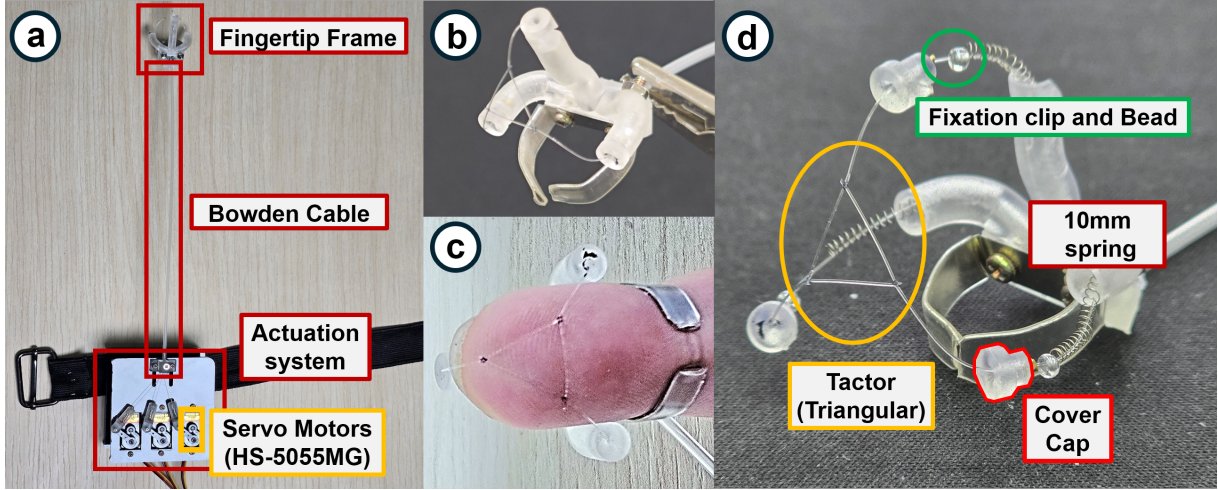


Figure 2: (a) Implementation and appearance of StringTouch. (b) Tactor mounted on the fingertip frame. (c) Placement of the tactor(triangular) on the fingertip. (d) Close-up view of the frame and its components.

to the fingertip, and an actuation part that independently controls the tension in three strings. Figure 2(a) illustrates each component's detailed configurations and terminologies, described below.

3.2.1 Fingertip frame. To securely mount the selected string structure, we designed a 3D-printed claw-shaped frame attached to the fingertip, produced in three sizes matching the triangular structure. The claw has three tubes that connect to the Bowden cable at each location, and inside the tube, beads and 10 mm length springs are fixed to the string, creating a restoring force against the force of the motor pulling the string. The range in which the beads can move inside each tube is 7 mm, which is applied larger than the maximum movement range of the string structure used throughout the experiment. At the lower part of the frame, a thin, bendable metal plate can be secured with bolts near the distal finger joint, ensuring stable attachment and reducing unwanted movement.

3.2.2 Bowden cable. We used a Bowden cable structure consisting of the same nylon string and a flexible plastic tube (150 mm in length, 2 mm in thickness) to transmit power from the remote actuators to the fingertip-mounted structures. This minimizes hand encumbrance and preserves VR hand-tracking compatibility.

3.2.3 Actuation system. Three HS-5055MG servo motors (Hitec), powered at 5 V DC and controlled by an Arduino Leonardo, actuate each string independently. Each motor provides a maximum torque of approximately 1.3 kg·cm, sufficient to induce skin deformation given that previous studies reported saturation of skin deformation at normal direction around 3 N [41]. A potentiometer adjusts the string offset simultaneously (counterclockwise to tighten, clockwise to loosen). At the loosest setting, the tactor maintained a 1–2 mm clearance beyond the finger's thickness for easier mounting. This tension adjustment was also used for initial calibration after wearing StringTouch, ensuring the tactor lightly touched the finger.

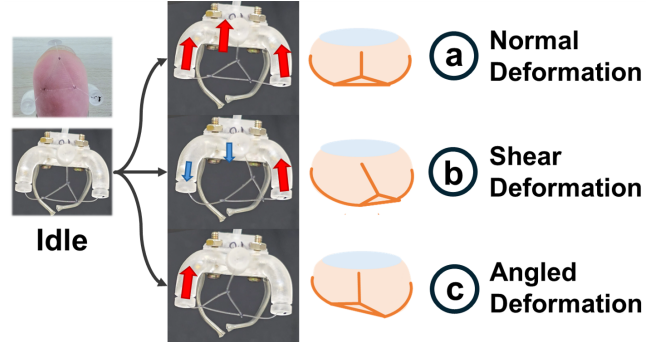


Figure 3: Types of finger deformation driven by StringTouch. (a) Normal, (b) Shear (left shear in figure), and (c) Angled (right angled in figure) deformation. The arrows indicate the directions and magnitudes in which the strings are pushed or pulled.

3.3 Actuation Type and Mechanism

StringTouch utilizes the described mechanical structure and string tactor, and each motor applies sufficient string-pulling force at the end of the frame (2.36 N). Each tactor motor controlled the string with 0.2 mm precision, requiring 0.11 seconds for maximum displacement. The distance the string moves at the fingertip frame is approximately two-thirds of the distance pulled by the motor—for example when the motor pulls the string by 6 mm, the string at the fingertip frame moves by 4 mm. This difference in displacement is caused by factors such as friction and movement of the string within the Bowden cable, as well as slight compression or deformation of the cable itself. Three distinct deformation modes were implemented to achieve diverse sensory modulation.

3.3.1 Normal deformation. All three motors simultaneously pull strings equally, vertically pulling the fingertip skin. This mode

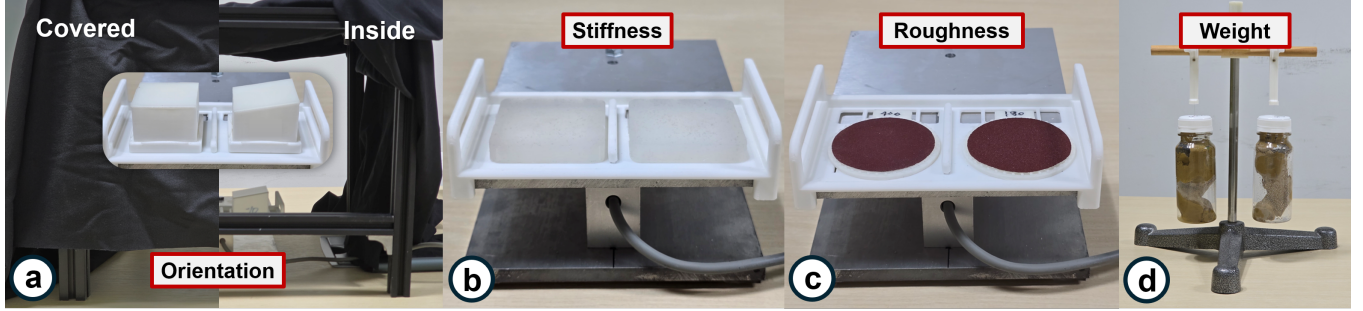


Figure 4: Experimental setup for User Study 1. (a) Object setup for the Orientation task (left: covered with fabric, right: internal view without fabric), (b) Setup for the Stiffness task, (c) Setup for the Roughness task, (d) Setup for the Weight task. All tasks were conducted with the setup covered in fabric, as shown in (a)

is expected to modulate perceived stiffness [45, 50] or increase perceived grip force [26], altering object weight perception. For stiffness, when the string tacter presses the finger, the rest of the fingerpad becomes bulgier, increasing the contact area with the object. This aims to make the object feel softer, similar to the principle used by Tao et al.'s device [50].

3.3.2 Shear deformation. Differential pulling of the motors translates the central contact point within the fingertip plane, inducing directional shear deformation. The translation was calculated using barycentric coordinates with the triangle formed by the frame as vertices. This mode aims to modulate perceived object weight by simulating directional skin pressure, either along or against the direction of gravity [28].

3.3.3 Angled deformation. Selective pulling from a single motor direction tilts the contact plane, creating angled deformation of the fingertip. This deformation is for altering the perceived angle of objects during touching. Several studies have shown that the perceived orientation can be changed by tilting the plane on which the finger touches the surface [48].

4 User Study 1: Experimental Validation of Tactile Occlusion under Varying Occluding Conditions

This experiment addresses RQ1 by examining tactile sensitivity variations under different fingertip occlusion methods, particularly assessing how sensory discrimination is preserved with the string structure compared to bare fingers. Twelve right-handed participants (8 males, 4 females; age: $M = 22.7$, $SD = 2.38$) participated.

4.1 Experimental Setup

We measured discrimination thresholds for four tactile properties (**Weight**, **Stiffness**, **Roughness**, **Orientation**) across four occlusion conditions: bare finger, Y-shaped string (*Yshape*), triangular string (*Triangular*), and a latex finger cot (*Masked*). These tactile properties were selected based on previous studies of fingertip occlusion (roughness [32]) and the specific tactile sensations our device targets (weight, orientation, stiffness). The experimental setup is shown in Figure 4. The detailed conditions are as follows:

4.1.1 Occlusion conditions. 3D-printed fingertip-mounted guides (shown in Figure 5(a)) were fabricated for the string conditions to provide constant fingertip tension (1 N–1.1 N), measured using a tension gauge. This tension ensured slight fingertip deformation without the tacter slipping from the skin. The structures matched the cover positions shown in Figure 2(c), with springs attached at the ends of each string to generate consistent tension when worn. 3D-printed spacers (width 1.0 mm to 2.6 mm, increments of 0.2 mm) were used to standardize tension across varying participant finger thicknesses. The *Masked* condition used a 0.1 mm latex finger cot to assess the effects of whole fingertip occlusion.



Figure 5: (a) Occlusion conditions for User Study 1: Spacer, Y-shaped tacter (*Yshape*), Triangular tacter (*Triangular*), and latex finger cot (*Masked*). (b) Participants wore an acrylic sheath on their thumb during the Weight experiment.

4.1.2 Stimuli sets. Participants compared reference and variable stimuli randomly presented in pairs:

- **Orientation:** 3D-printed blocks (4 cm x 4 cm) covered with Teflon tape; reference at 0° (horizontal), with test angles $\pm 0.5^\circ$, $\pm 1^\circ$, $\pm 3^\circ$, $\pm 4^\circ$, $\pm 5^\circ$, $\pm 10^\circ$, $\pm 15^\circ$. A positive angle means a block tilted counter-clockwise (ccw), and a negative angle means a block tilted clockwise (cw). This stimulus set refers to the previously performed discrimination task [42].
- **Stiffness:** Silicone plates made by mixing several liquid silicones (MK-MoldMaster; ShoreA-5, 12, 20, 25, 40) in various mixing ratios, with size of 50×50×7.5 mm; reference stiffness

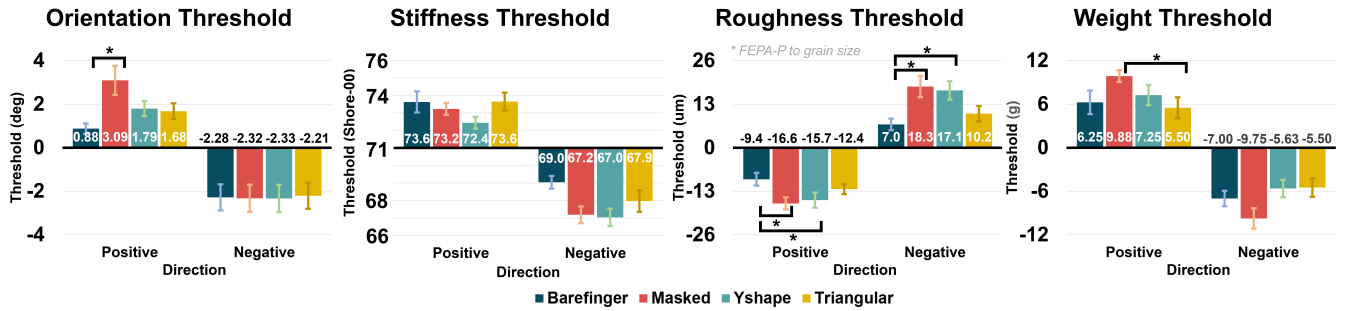


Figure 6: The results of the discrimination thresholds under each occlusion condition for the four experiments (in order: Orientation, Stiffness, Roughness, and Weight). Error bars represent standard errors, and asterisks indicate statistically significant differences (*: $p < .05$).

(average) shore00-71, positive (harder): 73, 74, 75, 76, 79 and negative (softer): 69, 67, 65, 64, 63. Each stiffness was measured with a Shore00 durometer at 10 points and averaged. Every point had a gap within ± 1 from the average.

- **Roughness:** Circular sandpapers (diameter 50 mm); reference grit 400, positive (smoother): 600, 800, 1000, 2000 and negative (rougher): 320, 240, 180, 120. This corresponds to a softer range than the previous roughness discrimination test [32] and was intended to reflect the roughness of objects commonly encountered daily.
- **Weight:** Plastic bottle (diameter 47 mm) filled with clay; reference weight 200 g, increments ± 6 g (range: 170–230 g).

4.2 Procedure

Except for **Weight**, experiments were conducted at a platform ($W \times H: 80 \text{ mm} \times 140 \text{ mm}$) equipped on a load cell (CAS BCA-10L) to prevent participants from estimating stiffness based on how deeply their finger bones pressed into the plate under excessive force (Figure 4(a-c)). For **Weight**, bottles were hung from both sides of the stand using nylon threads attached to their caps, allowing participants to grasp and lift them (Figure 4(d)). The hanger's structure restricted the lifting distance to less than 1 cm, limiting the ability to perceive weight through inertia. For each occlusion condition, participants wore the corresponding equipment (Figure 5(b)) on the index finger of their dominant hand.

Each occlusion condition was counterbalanced for the subjects, and the discrimination experiment followed the sequence: **Orientation** → **Stiffness** → **Roughness** → **Weight**.

A minimum of 5 minutes of rest was guaranteed between each experiment. Participants placed their dominant hand inside a box covered with blackout fabric. Two randomly placed stimuli objects (reference and variant) were presented, and participants interacted for up to 10 seconds before verbally identifying the more "tilted/hard/rough/heavy" object. In the **Orientation** discrimination experiment, participants were asked to recognize the angle by pressing the top of the block with their index finger without stroking it while positioning their arm at a height parallel to the angle block. In the **Stiffness** discrimination experiment, participants were asked to distinguish stiffness by pressing the silicone with a force of less than 3 N, and an alarm was set to sound when pressing

with an excessive force. In the **Roughness** discrimination experiment, participants passively placed their finger on the sandpaper without rubbing to assess static roughness perception through skin deformation, not friction. In the **Weight** discrimination experiment, participants were asked to distinguish weight by lifting and holding the bottle slightly using their thumb and index finger. They wore a sheath made of acrylic plate coated with a nonslip sticker to prevent discrimination with the sensation of the thumb (Figure 5(b)).

The experiment proceeded with a 1-down-1-up double-interlaced staircase for all cases, with the initial condition starting three steps from the reference object. The step between the stimulus and reference for the next trial was increased or decreased depending on whether the trial was correct. One session was conducted until there were 5 reversals each for both directions, and the discrimination threshold was calculated using the last 4 reversal response values. The experiment lasted approximately 120 minutes per participant.

4.3 Result and Discussion

4.3.1 Orientation. Orientation discrimination thresholds are presented in Figure 6. The results showed asymmetry between the positive (ccw-tilted) and negative (cw) directions. We speculate that this is due to the slight clockwise wrist rotation common in a pronated arm posture [38], causing participants to perceive the reference horizontal orientation as slightly tilted, especially without visual feedback. Since Shapiro-Wilk tests indicated non-normal distributions in both positive and negative directions, Friedman tests were conducted. The results showed a significant difference among occlusion conditions for the positive direction ($X^2 = 12.025, p = .007$). Conover's posthoc test with Bonferroni correction indicated a significant difference between the barefinger and *Masked* conditions ($p = .011$). No significant differences were observed for the negative direction. These results show that in the positive direction, both string conditions showed non-significant discrimination thresholds compared to the bare finger, while the finger cot significantly reduced orientation discrimination ability. This indicates both string structures can maintain sufficient fingertip tactile sensitivity for orientation perception.

4.3.2 Stiffness. Stiffness discrimination thresholds are shown in Figure 6. Shapiro-Wilk tests indicated normality in both directions; thus, repeated-measures ANOVAs (RM-ANOVA) were performed.

No significant differences emerged for the positive direction (stiffer), while a significant difference was observed in the negative direction (softer) ($F(3, 33) = 3.153, p = .038$). However, subsequent Bonferroni-corrected post-hoc comparisons revealed no significant pairwise differences. These results indicate that occlusion conditions influenced discrimination for softer stimuli (below Shore00-71), with the lowest mean threshold observed for the *Yshape*.

Some participants (3 of 12) reported that the *Yshape* directly covered the fingertip's central contact point, making silicone stimuli feel softer. This feedback, together with threshold results, indicates that covering the central area of the fingertip affects the perception of stiffness.

4.3.3 Roughness. Due to the vast and nonlinear FEPAP range (P180–P2000) used in the roughness analysis converted values into corresponding average grain sizes [36].

Roughness discrimination thresholds are presented in Figure 6. Shapiro-Wilk tests confirmed normality in both positive and negative directions; therefore, RM-ANOVA was used to test significance in occlusion conditions. For the positive (smoother) direction, thresholds differed significantly according to the occlusion condition ($F(3, 33) = 4.456, p = .010$). Post-hoc paired-sample t-tests with Bonferroni correction revealed significantly increased discrimination thresholds for the *Yshape* ($p = .047$) and *Masked* conditions ($p = .015$) compared to barefinger. Likewise, significant differences were observed in the negative (rougher) direction ($F(3, 33) = 4.982, p = .006$). Post-hoc tests similarly showed significantly increased thresholds for *Yshape* ($p = .036$) and *Masked* ($p = .015$) conditions compared to barefinger.

These findings indicate that the triangular-shaped string tactotactile sensitivity for roughness discrimination than the *Yshape* and *Masked* condition.

4.3.4 Weight. Weight discrimination thresholds are illustrated in Figure 6. Friedman tests were conducted as normality was violated in positive and negative directions. A significant difference appeared for the positive (heavier) direction ($X^2 = 9.391, p = .025$). Conover's post-hoc tests (Bonferroni-corrected) indicated a significant difference between *Triangular* and *Masked* conditions ($p = .042$). The negative direction also showed significance ($X^2 = 8.236, p = .041$), but post-hoc comparisons revealed no specific significant pairs.

Both string conditions showed a non-significant difference from bare finger performance, while the *Masked* condition significantly impaired discrimination compared to the *Triangular*.

Based on findings from the four experiments, we selected the triangular-shaped tactotactile for subsequent studies. The discrimination ability of the triangular tactotactile is better than that of other occlusion conditions, while the triangular planar shape is expected to enhance directional tactile modulation more than the Y-shaped tactotactile.

5 User Study 2: Experimental Validation of Sensory Modulation by StringTouch

This experiment aimed to validate the ability of StringTouch to modulate perceived sensations (**Weight, Stiffness, Orientation**) based on its deformation type and intensity. Twelve right-handed participants (10 males, 2 females; age: M = 22.1, SD = 2.4) took part.

5.1 Stimuli Given by StringTouch

The three deformation methods described in Section 3.3 were used to represent distinct tactile sensations: Normal and shear deformations for weight perception, normal deformations for stiffness perception, and angled deformation for orientation perception. The maximum displacement length for each deformation was as follows. The length corresponds to the distance the motor pulled the string, not the distance the string structure passed through the cable pulled. The relationship between them can be found in Section 3.3.

- **Normal Deformation:** All three motors simultaneously pulled the strings upward by up to 6 mm, creating uniform vertical skin deformation.
- **Shear Deformation:** One motor (left or right; from, dorsal side of the finger) pulled the string by 4.5 mm, while the remaining two motors released the string by 1.5 mm each. This configuration provided planar shear deformation, creating lateral skin displacement combined with mild normal pressure, rather than the theoretical operating value (+4.5 mm / -2.25 mm / -2.25 mm) in barycentric coordinates.
- **Angled Deformation:** One motor (left or right, from dorsal side of the finger) pulled the string by up to 6 mm, resulting in asymmetric angular deformation on the fingertip skin.

Additionally, we included intermediate intensities (1/3 and 2/3 of the maximum string displacement) to assess perceptual changes relative to deformation magnitude. All participants were pre-tested with these stimuli and reported no pain or discomfort.

5.2 Experimental Setup

Participants conducted the experiment using the same black-out box used in User Study 1, wearing noise-canceling headphones to mask actuator sounds. Each experiment had three reference objects to determine whether the degree of perceptual shifts was relative or absolute according to the reference value.

5.2.1 Weight. A PHANTOM Omni device [47] dynamically adjusted perceived weight (Figure 7(a)). Its stylus tip was connected via nylon thread beneath the platform to a cylindrical bottle with a holder (47 mm diameter). Reference weights were set at 100g, 200g, and 300g, with an additional 80g provided by *Omni* (thus, bottle and holder weights were calibrated at 20g, 120g, and 220g). Participants experienced nine stimuli combinations of three stimuli (left and right shear, normal deformation) and three intensity levels. The string connecting the stylus tip to the bottle was lubricated to minimize friction, allowing direct force transmission from the *Omni*.

5.2.2 Stiffness. Due to difficulty in continuous stiffness modulation, 13 discrete silicone samples (Shore00-63, 64, 65, 67, 69, 71, 73, 74, 75, 76, 79, 82, 85) were mounted on a rotating platform (Figure 7(b)). The reference objects were set to shore00 67, 74, and 79. Participants evaluated three intensities of normal deformation, totaling three stimulus conditions.

5.2.3 Orientation. In the case of angle, a structure that could rotate in 1° increments clockwise or counterclockwise to the front as a reference axis was prepared using a servo motor, a 5mm acrylic plate, and a PCB supporter (Figure 7(c)). Reference angles used were 0°: parallel to the floor, ±20°: tilted 20° cw(negative)/ccw(positive).

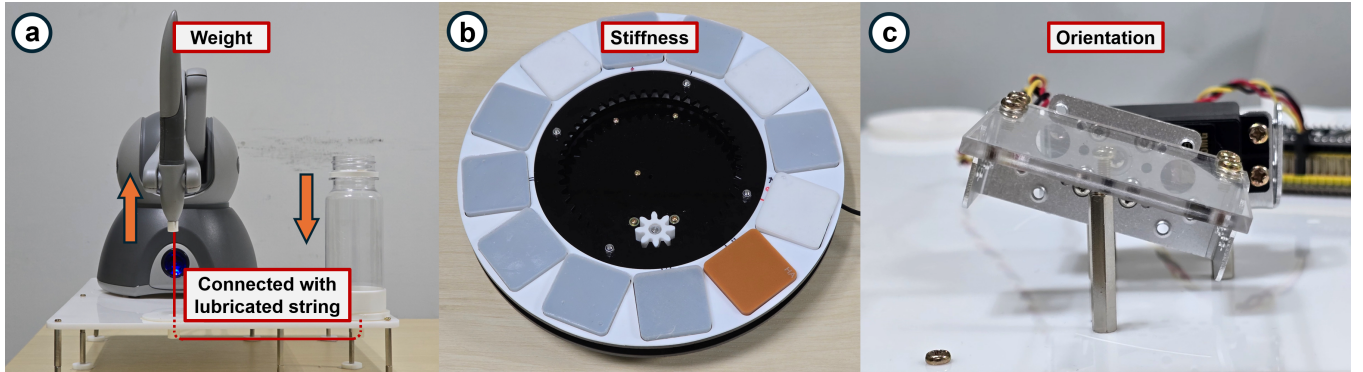


Figure 7: Experimental setup for User Study 2. (a) A PHANToM Omni device and bottles (filled with clay in the experiment) for weight modulation measurement. The nylon string at the bottom is highlighted (red). (b) A rotating disc with silicone plates is used to measure stiffness modulation. (c) An acrylic plate is connected to the servo motor to measure orientation modulation. All tasks were conducted with the box covered in fabric.

The angle could be adjusted up to $\pm 20^\circ$ from the reference angle according to the user’s operation. In the **Orientation** experiment, left or right-angled deformations were applied at three intensity levels, totaling six combinations.

5.3 Procedure

Participants wore the StringTouch device on their dominant hand index finger, placed inside the blackout enclosure. Experiments proceeded sequentially (**Weight** \rightarrow **Stiffness** \rightarrow **Orientation**), repeating each session across the three counterbalanced reference objects. Participants were able to toggle the stimulus on/off by pressing the space bar on the keyboard with their left hand, interact with the reference without StringTouch stimuli, and adjust the weight/stiffness/orientation values using the left and right arrow keys until they felt the same as the sensation generated when stimuli were provided. Participants were instructed to interact with each object (bottle, silicone, angle) in the same manner as in User Study 1. The manipulating values for a step were set as **Weight**: ± 3 g (maximum ± 80 g), **Stiffness**: neighboring stiffness plate, and **Orientation**: $\pm 1^\circ$. After adjustment, they could proceed with the same process for the next stimulus with the enter key. Each stimulus combination was repeated twice, randomized within a session (total **Weight**: 18 trials; **Stiffness**: 6 trials; **Orientation**: 12 trials per session.) The experiment took approximately 120 minutes per participant.

5.4 Result and Discussion

For **Weight** and **Orientation** experiments, two-way RM-ANOVAs (*Intensity* \times *Reference object*) were conducted to identify if sensory modulation was absolute or relative to the reference. Shapiro-Wilk tests indicated normality violations; thus, RM-ANOVA was conducted using aligned-rank transform [52]. For **Stiffness**, tests were separately performed for reference due to the non-linear Shore00 scale, employing Friedman tests due to normality violations.

5.4.1 Weight.

Responses are presented in Figure 8. **Left shear deformation:** Significant main effects were observed for *Intensity* ($F(1.19, 11.91) = 4.939, p = .041$) and *Reference object*

($F(2, 20) = 4.067, p = .033$). No significant interaction occurred. Bonferroni-corrected post-hoc tests revealed Level 3 induced significantly greater modulation than Level 1 ($p = .031$). Wilcoxon tests indicated no significant differences across reference weights.

Right shear deformation: Significant effects emerged only for *Intensity* ($F(2, 22) = 21.766, p < .001$). Post-hoc tests showed significant progressive increases in perceived weight across all intensity levels (Level 1–2: $p = .018$; Level 1–3: $p < .001$; Level 2–3: $p = .045$), suggesting intensity-dependent weight modulation.

Normal deformation: *Intensity* significantly affected perceived weight ($F(2, 22) = 14.166, p < .001$), with significant increases between Levels 1–3 ($p < .001$) and Levels 2–3 ($p = .021$). No significance for *Reference* or interaction was observed.

In conclusion, right shear and normal deformation robustly induced heavier perceptions regardless of reference weights, while left shear deformation varied depending on the reference. Additionally, the left shear’s average modulation was lower, possibly because deformations against gravity are inherently less effective than those aligned with gravity.

5.4.2 Stiffness. Responses (Figure 9) indicated significant difference on *Intensity* for the stiffest reference (Shore00-79; $X^2 = 8.450, p = .015$), with Level 1–3 differing ($p = .023$). Generally, participants perceived stimuli as softer with deformation, with modulation intensity dependent on stiffer references. However, two participants exhibited the opposite effect (perceived stiffer). Excluding these participants, significance according to *Intensity* appeared for all references (Shore00-67: $X^2 = 11.706, p = .003$; Shore00-74: $X^2 = 10.757, p = .005$; Shore00-79: $X^2 = 10.757, p = .005$), with Level 1–3 pairs consistently significant ($p < .01$). Thus, normal deformation typically reduced perceived stiffness, though individual differences in response direction were noted.

5.4.3 Orientation.

Results are shown in Figure 10. **Right angled deformation:** Significant *Intensity* effects were found ($F(2, 22) = 10.911, p < .001$), with significant differences between Levels 1–3 ($p = .004$) and Levels 2–3 ($p = .042$). No reference effect or interaction emerged.

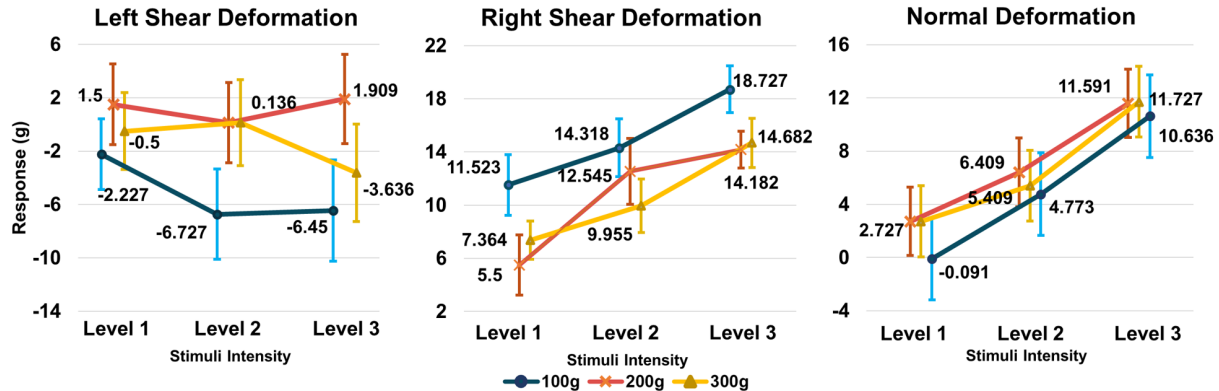


Figure 8: Weight modulation responses according to stimuli intensity (x-axis) and reference object (lines). Error bars represent standard errors.

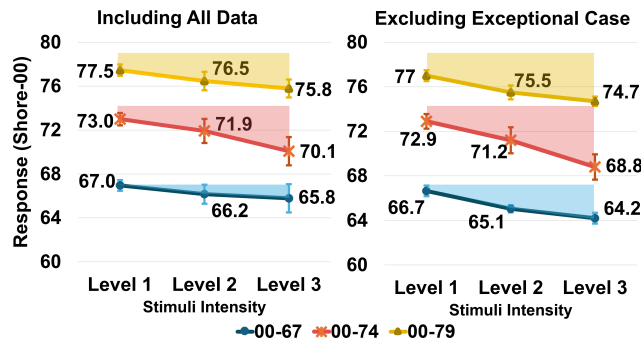


Figure 9: Stiffness modulation responses according to stimuli intensity (x-axis) and reference (lines). Error bars indicate standard errors. Shaded areas along each line indicate the amount of deviation from the corresponding reference.

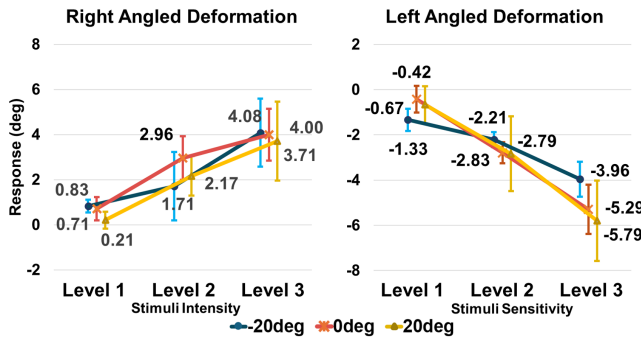


Figure 10: Orientation modulation responses according to stimuli intensity (x-axis) and reference object (lines). Error bars represent standard errors.

Left angled deformation: Highly significant *Intensity* effects appeared ($F(2, 22) = 44.600, p < .001$), with significant pairwise differences among all levels (Levels 1–2: $p = .009$, Levels 1–3: $p = .003$, Levels 2–3: $p = .004$).

Increased deformation intensity consistently enhanced angular modulation independent of reference angle. Comparisons between deformation directions (left/right) at each intensity level using the Wilcoxon test also showed no significant differences.

6 User Study 3: Interacting with Tangible Proxies in VR

This experiment addresses RQ3, evaluating whether StringTouch offers a more realistic VR interaction experience than a barehand condition when using tangible proxies. Ten right-handed participants (9 males, 1 female; age: $M = 23.5, SD = 1.7$) participated, including two from User Study 2; all had prior VR experience. Each participant tested two conditions (barehand vs. StringTouch) across three scenarios corresponding to the sensations (Weight, Stiffness, Orientation) validated in User Study 2. Participants rated realism using a 7-point Likert scale (1: not realistic, 7: realistic) and indicated their preferred condition. Conditions were counterbalanced, with brief interviews after each scenario. The experiment lasted approximately 60 minutes per participant.

6.1 Scenario and Proxy Setup

The experiment was conducted using Meta Quest 3, utilizing its native hand-tracking. Setup for each scenario is shown in Figure 11. Each proxy was mounted on a 3D-printed platform (W: 250 mm × H: 50 mm), connected to a load cell to check whether the user was calibrating their position in the VR or interacting with the proxy based on the force applied. Two PCB support columns (height: 130 mm) attached to each side held cylindrical handles (height: 70 mm, diameter: 34 mm) for initial hand calibration at the scenario start. The load cell also detected whether the user was interacting with the proxy by monitoring weight changes (lifting a bottle, pressing a bear, stroking a cylinder), and activated the device. At the start of the scene, users calibrated the position by grasping the handles with hands and pressing down. The proxies and deformation stimuli for each scenario are as follows:

6.1.1 Scenario 1: Pouring water into a cup using weight modulation. Participants interacted with a cylindrical proxy bottle (diameter: 47 mm). Upon grasping the proxy with their thumb and index

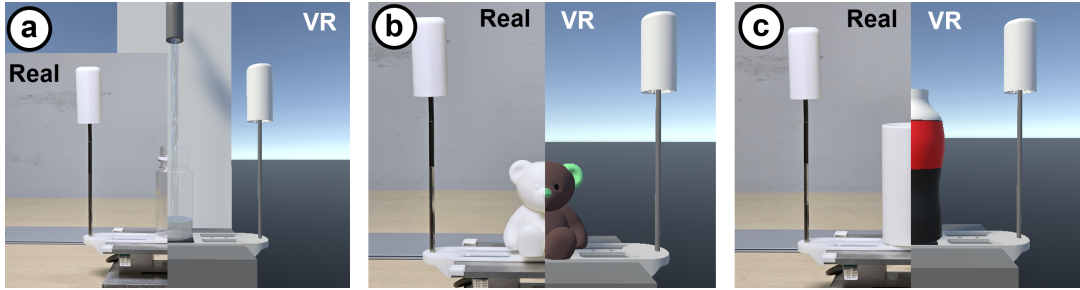


Figure 11: Experimental setup for User Study 3. Images were composed by splitting the actual setup in half, with the physical proxy shown on the left and the virtual environment on the right: (a) Scenario 1, (b) Scenario 2, (c) Scenario 3.

finger, a virtual bottle synchronized with the participant's hand movements. In the StringTouch condition, as participants filled the virtual bottle from a virtual faucet, right-side (downward) shear deformation (same maximum intensity from Study 2) increased linearly in proportion to the water level, accompanied by visual feedback of rising water. Participants could reset the water by returning the bottle to its original position.

6.1.2 Scenario 2: Touching a teddy bear using stiffness modulation. Participants interacted with a 3D-printed teddy bear (height: approximately 90 mm). The virtual environment displayed an identical bear, highlighting the nose and ears in green. Participants were informed beforehand that the virtual bear had a rigid plastic nose and felt-filled body. Participants freely pressed these marked areas with their index fingers. In the StringTouch condition, maximum normal deformation (from Study 2) is triggered by pressing the ears and resets on release. In both conditions, visual feedback included gradual color shifts from green to red and flattening mesh deformation proportional to finger pressure for ear press.

6.1.3 Scenario 3: Stroking a bottle using orientation modulation. Participants used a cylindrical 3D-printed proxy (height: 127 mm, diameter: 60 mm) while virtually stroking a bottle with curved surfaces. The virtual bottle featured a straight lower section (25 mm, matching proxy diameter), a concave middle (50 mm), and a convex upper section (50 mm). The maximum radius difference was 6 mm, creating slopes up to approximately 9°. In the StringTouch condition, angled deformation proportionally matched the local slope (maximum deformation from Study 2 scaled by slope angle relative to the 9° maximum). The participant's finger movements were visually retargeted in VR to align with the curved surfaces.

6.2 Result

Since the normality assumption was violated, a Friedman test was used for presence scores across device conditions. Presence scores and preference results (Figure 12) showed significantly higher presence for StringTouch in all scenarios (Scenario 1: $X^2 = 6.400$, $p = .011$; Scenario 2: $X^2 = 10.000$, $p = .002$; Scenario 3: $X^2 = 10.000$, $p = .002$), with over 70% participants preference in each scenario.

6.3 Qualitative Feedback

Across all scenarios, StringTouch provided a greater presence in VR proxy interactions. However, several participants felt the difference

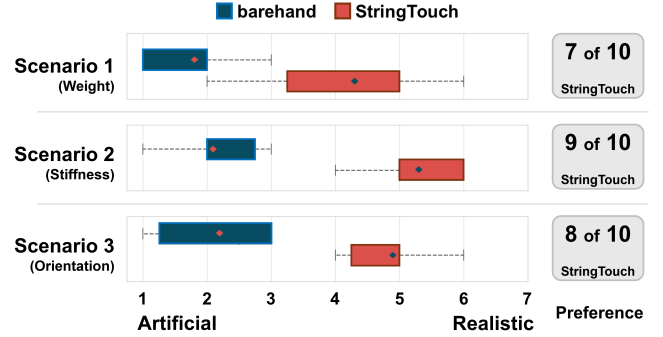


Figure 12: Realism and preference across all participants for three scenarios. Graphs indicating realism score include average (dot), IQR, and min/max.

in presence between the two conditions was minimal, leading some to prefer the barehand condition.

6.3.1 Feedback on Scenario 1. In the scenario where participants filled a virtual bottle with water, those who preferred the StringTouch condition (P1, P3, P4, P7, P8, P9, P10) mentioned increased realism from feedback simulating continuous weight gain. However, some participants (P1, P3, P7) felt the sensation was incomplete due to the absence of increased load on the hand or arm. For instance, P1 stated: “*It felt realistic because the object seemed heavier, causing my fingers to grip tighter, but I didn’t perceive additional weight when moving my hand or arm.*” Conversely, participants who preferred the barehand condition cited discrepancies between visual and tactile sensations (P2, P5) and the localized nature of tactile feedback (P6). Specifically, P2 commented: “*When gripping the object while it was filling with water, the stimulation at my fingertip made it feel as if the object was expanding rather than becoming heavier.*” P6 added: “*If an object becomes heavier, I expect increased force across my entire hand, but the sensation was limited to just the single fingertip, causing a mismatch.*” These results indicate room for improvement in the naturalness of weight modulation.

6.3.2 Feedback on Scenario 2. In the scenario where participants alternately touched two virtual objects with different stiffnesses, nine participants (P1, P2, P3, P4, P5, P6, P7, P9, P10) preferred the StringTouch condition, highlighting distinct sensations between

materials. P3 remarked: “*I pressed the same material each time, yet it felt different depending on where I pressed. The fingertip deformation created an impression of greater compressibility.*” The participant who preferred the barehand condition (P8) agreed that the stiffness differences were noticeable but expressed concerns about realism: “*The momentary activation of the device before touching the object felt unrealistic. Visual cues (the object visually deforming) provided sufficient realism, so the device wasn’t worth wearing.*”

6.3.3 Feedback on Scenario 3. In the scenario involving stroking bottle with varying curvatures, eight participants (P1, P3, P4, P5, P7, P8, P9, P10) preferred the StringTouch, agreeing that the tactile deformation matched the virtual object’s surface angles. Participant P9 mentioned: “*For gently curved areas, tactile changes felt subtle, but angle variations in sharply curved regions were much clearer.*” The two participants who preferred the barehand condition (P2, P6) acknowledged tactile modulation but felt the device’s advantages did not outweigh its drawbacks. P2 stated: “*The additional tactile sensation did increase realism, but the visual feedback alone (seeing the finger tracing curved surfaces) was sufficient, making the device unnecessary.*” Similarly, P6 commented: “*I actually found it more realistic when receiving tactile stimulation in mid-air, without touching the cylindrical proxy. The flat tactile feedback of the proxy surface conflicted with attempts to simulate curvature changes. I think it’s maybe due to the narrow stimuli region, not simulating whole hand.*”

7 General Discussion and Future Work

7.1 RQ1: StringTouch’s Tactor Maintained Sensory Discrimination Ability

User Study 1 revealed significant masking effects with the latex finger cot for orientation, roughness, and weight sensations. Among the nylon-string tactors, the Y-shaped tactor notably masked roughness discrimination. In contrast, the triangular-shaped tactor showed no significant masking effect compared to the bare finger for all tested sensations. Specifically, the triangular tactor demonstrated superior weight discrimination sensitivity compared to the finger cot, with the lowest discrimination threshold among occlusion conditions. These findings align with previous studies highlighting enhanced finger sensitivity using less-occlusive tactors [18, 51, 56], indicating the effectiveness of the open fingertip area in preserving sensory discrimination. Interestingly, despite covering less skin than the triangular tactor, the Y-shaped tactor significantly masked roughness discrimination. One participant noted during the experiment: “*When I press with my finger to distinguish the roughness, the string on my finger touches the sandpaper first, so I can’t really feel the texture properly.*” Based on such feedback, we speculate the triangular shape facilitated roughness discrimination by enabling direct fingertip contact, whereas the Y-shaped tactor may have hindered sensitivity by covering the critical contact zone.

7.2 RQ2: StringTouch Provides Effective Tactile Cues for Weight, Stiffness, and Orientation

User Study 2 results showed that right shear deformation at maximum intensity increased perceived weight by approximately 14–19 g across reference weights (100 g, 200 g, 300 g). Similarly, normal deformation reduced perceived stiffness by about 3–6 units

(Shore00), and angled deformation produced orientation shifts of approximately 3–5°. These findings are consistent with previous studies on tactile modulation using skin deformation (Weight [28], Stiffness [50]), demonstrating that StringTouch can modulate tactile properties through fingertip deformation, even without visual cues.

However, several participants (4 of 12) perceived all stimuli (left shear, right shear, and normal deformation) as increasing weight, regardless of intended direction. Specifically, left shear deformation, designed to reduce perceived weight, showed weaker modulation and less consistent influence across reference weights. This contrasts with prior studies using fingerpad skin shear stretch for weight modulation. Choi et al.’s Grability [7] successfully altered perceived weight in both directions through asymmetric vibrations that stretched the skin at different speeds in upwards and downwards. StringTouch’s weaker negative weight modulation may result from shear deformation inducing subtle pressure on the finger, producing tactile effects similar to normal deformation. It may also be related to gravity alignment, as noted in Section 5.4.1.

Tao et al. reported that perceived stiffness converged toward a specific value regardless of initial stiffness when applying similar skin deformation to our device [50]. However, our results showed a consistent downward shift in stiffness across various references instead of converging to a certain Shore value. This discrepancy likely arises from differences in stimulus ranges—our stiffest reference (Shore00-79) was approximately equal to the softest reference (ShoreA-40) in Tao et al.’s work, where similar perceptual shifts occurred—and the smaller deformation area of StringTouch.

7.3 RQ3: StringTouch Modulated Tactile Perceptions Enhancing Realism in VR Scenario using Tangible Proxies

We assessed presence and preference in three VR scenarios comparing barehand and StringTouch conditions with tangible proxies. Results indicated significantly higher presence ratings for StringTouch in all scenarios, with participant preference consistently above 70% (Scenario 1: 7/10; Scenario 2: 9/10; Scenario 3: 8/10). Additionally, qualitative feedback (Section 6.3) revealed that even participants preferring barehand interactions acknowledged that StringTouch increased interaction presence. These results indicate successful tactile modulation during proxy interactions with StringTouch.

However, our studies did not verify the effectiveness or independent applicability of simultaneous tactile modulations across multiple sensations (e.g., orientation and weight). For instance, User Study 1 showed that both right shear and normal deformation increased perceived weight, while normal deformation also influenced perceived stiffness. This suggests tactile cues altering softness might unintentionally influence weight perception. Future studies should examine whether tactile modulations can be independently controlled through visual cues or interaction context.

7.4 Future Enhancement for the StringTouch

Despite StringTouch’s overall positive feedback, some participants who preferred StringTouch noted that motor noise disrupted their immersive experience. This motor noise may be mitigated by replacing servo motors with quieter actuators like piezoelectric linear

motors. Participants favoring barefinger interaction mentioned limitations such as *localized tactile stimulation* (Scenario 1, 3) or *sudden device activation just before interacting with proxies* (Scenario 2).

To address the limited stimulation area, applying tactors across multiple fingers (thumb, index, middle, or more) could broaden the perceptual range, and multi-finger modulation with StringTouch may further enhance realism in dynamic interactions by simulating localized tilts or gravity per finger. Additionally, to deliver more realistic sensations across the whole hand—especially during varied grip postures such as a power grip—it may be beneficial to provide skin deformation to multiple finger joints (e.g., distal, middle, and proximal phalanges) [53]. In this case, to accurately determine fingertip contact and deformation directions, a more precise control algorithm responsive to finger-proxy interactions is required.

The unnatural sensation from sudden device activation may be mitigated by improving stimulus timing and actuation strategy. In our implementation of Scenario 2, maximum normal deformation was applied immediately upon contact for stiffness modulation. A more natural response may be possible by gradual deformation with pressing force. Further user studies are needed to explore parameters such as optimal timing and force-intensity mapping.

Additionally, the current StringTouch configuration, despite using only three motors per tactor, is already bulky enough to occupy wrist space; optimization in motor type, arrangement, and actuation mechanisms will be necessary to accommodate additional tactors without increasing device bulk. To avoid restricting hand and arm movement, integrating batteries with a low-power actuation design for wireless operation could further improve the device's usability.

8 Conclusion

We presented StringTouch, a non-occlusive 3DoF haptic device leveraging thin string structures to modulate fingertip sensations. Our user studies confirmed that the string-based tactors of StringTouch maintained finger sensory discrimination across diverse tactile sensations (Orientation, Stiffness, Roughness, and Weight). Furthermore, we experimentally demonstrated that StringTouch provided significant tactile cues for most users' weight, stiffness, and orientation perceptions. Lastly, applying StringTouch to VR interactions involving tangible proxies effectively altered perceived material properties, enhancing realism during proxy interactions. These findings suggest that StringTouch will be able to expand tangible proxies' expressive range and applicability, significantly broadening their potential use cases across VR/AR environments.

Acknowledgments

This work was supported by the National Research Foundation of Korea(NRF) grant funded by the Korea government. (MSIT) (RS-2024-00337679)

References

- [1] Mahdi Azmandian, Mark Hancock, Hrvoje Benko, Eyal Ofek, and Andrew D. Wilson. 2016. Haptic Retargeting: Dynamic Repurposing of Passive Haptics for Enhanced Virtual Reality Experiences. In *Proceedings of the 2016 CHI Conference on Human Factors in Computing Systems* (San Jose, California, USA) (*CHI '16*). Association for Computing Machinery, New York, NY, USA, 1968–1979. doi:10.1145/2858036.2858226
- [2] bHaptics. 2025. *TactGlove DK2*. Retrieved Apr. 2025 from <https://www.bhaptics.com/tactsuit/tactglove-dk2/>
- [3] Seda Bilaloglu, Ying Lu, Daniel Geller, John Ross Rizzo, Viswanath Aluru, Esther P Gardner, and Preeti Raghavan. 2015. Effect of blocking tactile information from the fingertips on adaptation and execution of grip forces to friction at the grasping surface. *J Neurophysiol* 115, 3 (Dec. 2015), 1122–1131.
- [4] A Bucknor, A Karthikesalingam, S R Markar, P J Holt, I Jones, and T G Allen-Mersh. 2010. A comparison of the effect of different surgical gloves on objective measurement of fingertip cutaneous sensibility. *Ann R Coll Surg Engl* 93, 2 (Nov. 2010), 95–98.
- [5] Lung-Pan Cheng, Eyal Ofek, Christian Holz, Hrvoje Benko, and Andrew D. Wilson. 2017. Sparse Haptic Proxy: Touch Feedback in Virtual Environments Using a General Passive Prop. In *Proceedings of the 2017 CHI Conference on Human Factors in Computing Systems* (Denver, Colorado, USA) (*CHI '17*). Association for Computing Machinery, New York, NY, USA, 3718–3728. doi:10.1145/3025453.3025753
- [6] Francesco Chinello, Monica Malvezzi, Domenico Prattichizzo, and Claudio Paccierotti. 2020. A Modular Wearable Finger Interface for Cutaneous and Kinesthetic Interaction: Control and Evaluation. *IEEE Transactions on Industrial Electronics* 67, 1 (2020), 706–716. doi:10.1109/TIE.2019.2899551
- [7] Inrak Choi, Heather Culbertson, Mark R. Miller, Alex Olwal, and Sean Follmer. 2017. Grability: A Wearable Haptic Interface for Simulating Weight and Grasping in Virtual Reality. In *Proceedings of the 30th Annual ACM Symposium on User Interface Software and Technology* (Québec City, QC, Canada) (*UIST '17*). Association for Computing Machinery, New York, NY, USA, 119–130. doi:10.1145/3126594.3126599
- [8] Inrak Choi, Yiwei Zhao, Eric J. Gonzalez, and Sean Follmer. 2021. Augmenting Perceived Softness of Haptic Proxy Objects Through Transient Vibration and Visuo-Haptic Illusion in Virtual Reality. *IEEE Transactions on Visualization and Computer Graphics* 27, 12 (2021), 4387–4400. doi:10.1109/TVCG.2020.3002245
- [9] Kiran Dandekar, Balasundar I Raju, and Mandayam A Srinivasan. 2003. 3-D finite-element models of human and monkey fingertips to investigate the mechanics of tactile sense. *J Biomech Eng* 125, 5 (Oct. 2003), 682–691.
- [10] Xavier de Tinguy, Claudio Paccierotti, Maud Marchal, and Anatole Lécuyer. 2018. Enhancing the Stiffness Perception of Tangible Objects in Mixed Reality Using Wearable Haptics. In *2018 IEEE Conference on Virtual Reality and 3D User Interfaces (VR)*, 81–90. doi:10.1109/VR.2018.8446280
- [11] L. Dominjon, A. Lécuyer, J.-M. Burkhardt, P. Richard, and S. Richir. 2005. Influence of control/display ratio on the perception of mass of manipulated objects in virtual environments. In *IEEE Proceedings. VR 2005. Virtual Reality*, 2005, 19–25. doi:10.1109/VR.2005.1492749
- [12] Martin Feick, Scott Bateman, Anthony Tang, André Miede, and Nicolai Marquardt. 2020. Tangi: Tangible Proxies For Embodied Object Exploration And Manipulation In Virtual Reality. In *2020 IEEE International Symposium on Mixed and Augmented Reality (ISMAR)*, 195–206. doi:10.1109/ISMAR50242.2020.00042
- [13] Martin Feick, Niko Kleer, Andre Zenner, Anthony Tang, and Antonio Krüger. 2021. Visuo-haptic Illusions for Linear Translation and Stretching using Physical Proxies in Virtual Reality. In *Proceedings of the 2021 CHI Conference on Human Factors in Computing Systems* (Yokohama, Japan) (*CHI '21*). Association for Computing Machinery, New York, NY, USA, Article 220, 13 pages. doi:10.1145/3411764.3445456
- [14] Martin Feick, Kora Persephone Regitz, Anthony Tang, and Antonio Krüger. 2022. Designing Visuo-Haptic Illusions with Proxies in Virtual Reality: Exploration of Grasp, Movement Trajectory and Object Mass. In *Proceedings of the 2022 CHI Conference on Human Factors in Computing Systems* (New Orleans, LA, USA) (*CHI '22*). Association for Computing Machinery, New York, NY, USA, Article 635, 15 pages. doi:10.1145/3491102.3517671
- [15] J R Flanagan, J Tresilian, and A M Wing. 1993. Coupling of grip force and load force during arm movements with grasped objects. *Neurosci Lett* 152, 1–2 (April 1993), 53–56.
- [16] Johann Felipe Gonzalez Avila, John C McClelland, Robert J Teather, Pablo Figueroa, and Audrey Girouard. 2021. Adaptic: A Shape Changing Prop with Haptic Retargeting. In *Proceedings of the 2021 ACM Symposium on Spatial User Interaction (Virtual Event, USA) (SUI '21)*. Association for Computing Machinery, New York, NY, USA, Article 4, 13 pages. doi:10.1145/3485279.3485293
- [17] Xiaochi Gu, Yifei Zhang, Weize Sun, Yuanzhe Bian, Dao Zhou, and Per Ola Kristensson. 2016. Dexmo: An Inexpensive and Lightweight Mechanical Exoskeleton for Motion Capture and Force Feedback in VR. In *Proceedings of the 2016 CHI Conference on Human Factors in Computing Systems* (San Jose, California, USA) (*CHI '16*). Association for Computing Machinery, New York, NY, USA, 1991–1995. doi:10.1145/2858036.2858487
- [18] David Gueorguiev, Bernard Javot, Adam Spiers, and Katherine J. Kuchenbecker. 2022. Larger Skin-Surface Contact Through a Fingertip Wearable Improves Roughness Perception. In *Haptics: Science, Technology, Applications*, Hasti Seifi, Astrid M. L. Kappers, Oliver Schneider, Knut Drewing, Claudio Paccierotti, Alireza Abbasimoshaei, Gijs Huisman, and Thorsten A. Kern (Eds.). Springer International Publishing, Cham, 171–179.
- [19] Anuruddha Hettiarachchi and Daniel Wigdor. 2016. Annexing Reality: Enabling Opportunistic Use of Everyday Objects as Tangible Proxies in Augmented Reality. In *Proceedings of the 2016 CHI Conference on Human Factors in Computing Systems* (San Jose, California, USA) (*CHI '16*). Association for Computing Machinery, New

- York, NY, USA, 1957–1967. doi:10.1145/2858036.2858134
- [20] H. G. Hoffman. 1998. Physically Touching Virtual Objects Using Tactile Augmentation Enhances the Realism of Virtual Environments. In *Proceedings of the Virtual Reality Annual International Symposium (VRAIS '98)*. IEEE Computer Society, USA, 59.
- [21] Mohsen Hosseini, Ali Sengül, Yudha Pane, Joris De Schutter, and Herman Bruyninck. 2018. ExoTen-Glove: A Force-Feedback Haptic Glove Based on Twisted String Actuation System. In *2018 27th IEEE International Symposium on Robot and Human Interactive Communication (RO-MAN)*. 320–327. doi:10.1109/ROMAN.2018.8525637
- [22] Brent Edward Insko. 2001. *Passive haptics significantly enhances virtual environments*. Ph.D. Dissertation. Advisor(s) Brooks, Frederick P. AAI3007820.
- [23] Peter Johnson and Janet Blackstone. 2007. Children and gender - Differences in exposure and how anthropometric differences can be incorporated into the design of computer input devices. *STWEH Supplements* 33 (01 2007).
- [24] Eun Kwon, Gerard J. Kim, and Sangyoon Lee. 2009. Effects of sizes and shapes of props in tangible augmented reality. In *2009 8th IEEE International Symposium on Mixed and Augmented Reality*. 201–202. doi:10.1109/ISMAR.2009.5336463
- [25] Tomosuke Maeda, Shigeo Yoshida, Takaki Murakami, Kenroh Matsuda, Tomohiro Tanikawa, and Hiroyuki Sakai. 2022. Fingeret: A Wearable FingertipPad-Free Haptic Device for Mixed Reality. In *Proceedings of the 2022 ACM Symposium on Spatial User Interaction* (Online, CA, USA) (*SUI '22*). Association for Computing Machinery, New York, NY, USA, Article 3, 10 pages. doi:10.1145/3565970.3567703
- [26] Maurizio Maisto, Claudio Pacchierotti, Francesco Chinello, Gionata Salvietti, Alessandro De Luca, and Domenico Prattichizzo. 2017. Evaluation of Wearable Haptic Systems for the Fingers in Augmented Reality Applications. *IEEE Transactions on Haptics* 10, 4 (2017), 511–522. doi:10.1109/TOH.2017.2691328
- [27] Sebastian Marichal, Iñigo Ezcurdia, Rafael Morales, Amalia Ortiz, Asier Marzo, and Oscar Ardaiz. 2023. Hand-as-a-prop: using the hand as a haptic proxy for manipulation in virtual reality. *Virtual Reality* 27, 4 (Dec. 2023), 2911–2925.
- [28] Kouta Minamizawa, Souichiro Fukamachi, Hiroyuki Kajimoto, Naoki Kawakami, and Susumu Tachi. 2007. Gravity grabber: wearable haptic display to present virtual mass sensation. In *ACM SIGGRAPH 2007 Emerging Technologies* (San Diego, California) (*SIGGRAPH '07*). Association for Computing Machinery, New York, NY, USA, 8–es. doi:10.1145/1278280.1278289
- [29] Neomi Mizrachi, Guy Nelinger, Ehud Ahissar, and Amos Arieli. 2022. Idiosyncratic selection of active touch for shape perception. *Scientific Reports* 12, 1 (feb 2022), 2922.
- [30] Philipp Moog, Manuela Schulz, Julia Betzl, Daniel Schmauss, Jörn A Lohmeyer, Hans-Günther Machens, Kai Megerle, and Holger C Erne. 2020. Do your surgical glove characteristics and wearing habits affect your tactile sensibility? *Ann Med Surg (Lond)* 57 (Aug. 2020), 281–286.
- [31] Peter Mylon, Matt J Carré, Nicolas Martin, and Roger Lewis. 2016. How do gloves affect cutaneous sensitivity in medical practice? Two new applied tests. *Proc Inst Mech Eng H* 231, 1 (Nov. 2016), 28–39.
- [32] Peter T Mylon, Luke Buckley-Johnstone, Roger Lewis, Matt J Carré, and Nicolas Martin. 2015. Factors influencing the perception of roughness in manual exploration: Do medical gloves reduce cutaneous sensitivity? *Proceedings of the Institution of Mechanical Engineers, Part J* 229, 3 (2015), 273–284. doi:10.1177/1350650113517111 arXiv:https://doi.org/10.1177/1350650113517111
- [33] Niels Christian Nilsson, André Zenner, and Adalberto L. Simeone. 2021. Propping Up Virtual Reality With Haptic Proxies. *IEEE Computer Graphics and Applications* 41, 5 (2021), 104–112. doi:10.1109/MCG.2021.3097671
- [34] Niels Christian Nilsson, André Zenner, Adalberto L Simeone, Donald Degraen, and Florian Daiber. 2021. Haptic proxies for virtual reality: Success criteria and taxonomy. In *Proceedings of the 1st Workshop on Everyday Proxy Objects for Virtual Reality (EPO4VR '21)*.
- [35] Aditya Shekhar Nittala, Klaus Kruttwig, Jaeyeon Lee, Roland Bennewitz, Eduard Arzt, and Jürgen Steimle. 2019. Like A Second Skin: Understanding How Epidermal Devices Affect Human Tactile Perception. In *Proceedings of the 2019 CHI Conference on Human Factors in Computing Systems* (Glasgow, Scotland Uk) (*CHI '19*). Association for Computing Machinery, New York, NY, USA, 1–16. doi:10.1145/3290605.3300610
- [36] Federation of European Producers of Abrasives. FEPA-ABRASIVES. 2025. *P-grit sizes coated*. Retrieved Apr. 2025 from https://fepa-abrasives.org/
- [37] Shuto Ogihara, Tomohiro Amemiya, and Kazuma Aoyama. 2022. Transcutaneous Electrical Nerve Stimulation along the Base of the Finger to Modify the Location of Tactile Sensation at the Finger. In *2022 IEEE International Symposium on Mixed and Augmented Reality Adjunct (ISMAR-Adjunct)*. 646–647. doi:10.1109/ISMAR-Adjunct57072.2022.000133
- [38] LW O'Sullivan and TJ Gallwey. 2005. Forearm torque strengths and discomfort profiles in pronation and supination. *Ergonomics* 48, 6 (2005), 703–721. doi:10.1080/00140130500070954 arXiv:https://doi.org/10.1080/00140130500070954 PMID: 16087504.
- [39] Claudio Pacchierotti, Gionata Salvietti, Irfan Hussain, Leonardo Meli, and Domenico Prattichizzo. 2016. The hRing: A wearable haptic device to avoid occlusions in hand tracking. In *2016 IEEE Haptics Symposium (HAPTICS)*. 134–139. doi:10.1109/HAPTICS.2016.7463167
- [40] Claudio Pacchierotti, Stephen Sinclair, Massimiliano Solazzi, Antonio Frisoli, Vincent Hayward, and Domenico Prattichizzo. 2017. Wearable Haptic Systems for the Fingertip and the Hand: Taxonomy, Review, and Perspectives. *IEEE Transactions on Haptics* 10, 4 (2017), 580–600. doi:10.1109/TOH.2017.2689006
- [41] D. T. V. Pawluk and R. D. Howe. 1999. Dynamic Lumped Element Response of the Human Fingertip. *Journal of Biomechanical Engineering* 121, 2 (04 1999), 178–183. doi:10.1115/1.2835100 arXiv:https://asmedigitalcollection.asme.org/biomechanical/article-pdf/121/2/178/5492394/178_1.pdf
- [42] Myrthe A. Plaisier, Loes C. J. van Dam, Catharina Gowania, and Marc O. Ernst. 2014. Exploration mode affects visuo-haptic integration of surface orientation. *Journal of Vision* 14, 13 (11 2014), 22–22. doi:10.1167/14.13.22 arXiv:https://arvojournals.org/arvo/content_public/jov/933685/11534-7362-14-13-22.pdf
- [43] Domenico Prattichizzo, Francesco Chinello, Claudio Pacchierotti, and Monica Malvezzi. 2013. Towards Wearability in Fingertip Haptics: A 3-DoF Wearable Device for Cutaneous Force Feedback. *IEEE Transactions on Haptics* 6, 4 (2013), 506–516. doi:10.1109/TOH.2013.53
- [44] Pornthep Preechayasonboon and Eric Rombokas. 2021. Haplets: Finger-Worn Wireless and Low-Encumbrance Vibrotactile Haptic Feedback for Virtual and Augmented Reality. *Frontiers in Virtual Reality* 2 (2021). doi:10.3389/fvr.2021.738613
- [45] Steeven Villa Salazar, Claudio Pacchierotti, Xavier de Tinguy, Anderson Maciel, and Maud Marchal. 2020. Altering the Stiffness, Friction, and Shape Perception of Tangible Objects in Virtual Reality Using Wearable Haptics. *IEEE Transactions on Haptics* 13, 1 (2020), 167–174. doi:10.1109/TOH.2020.2967389
- [46] HyunA Seo, Juheon Yi, Rajesh Balan, and Youngki Lee. 2024. GradualReality: Enhancing Physical Object Interaction in Virtual Reality via Interaction State-Aware Blending. In *Proceedings of the 37th Annual ACM Symposium on User Interface Software and Technology* (Pittsburgh, PA, USA) (*UIST '24*). Association for Computing Machinery, New York, NY, USA, Article 82, 14 pages. doi:10.1145/3654777.3676463
- [47] Alejandro Jarillo Silva, Omar A. Domínguez Ramírez, Vicente Parra Vega, and Jesús P. Ordaz Oliver. 2009. PHANTOM OMNI Haptic Device: Kinematic and Manipulability. In *2009 Electronics, Robotics and Automotive Mechanics Conference (CERMA)*. 193–198. doi:10.1109/CERMA.2009.55
- [48] Massimiliano Solazzi, Antonio Frisoli, and Massimo Bergamasco. 2010. Design of a novel finger haptic interface for contact and orientation display. In *2010 IEEE Haptics Symposium*. 129–132. doi:10.1109/HAPTIC.2010.5444667
- [49] Yudai Tanaka, Alan Shen, Andy Kong, and Pedro Lopes. 2023. Full-hand Electro-Tactile Feedback without Obstructing Palmar Side of Hand. In *Proceedings of the 2023 CHI Conference on Human Factors in Computing Systems* (Hamburg, Germany) (*CHI '23*). Association for Computing Machinery, New York, NY, USA, Article 80, 15 pages. doi:10.1145/3544548.3581382
- [50] Yujei Tao, Shan-Yuan Teng, and Pedro Lopes. 2021. Altering Perceived Softness of Real Rigid Objects by Restricting Fingertip Deformation. In *The 34th Annual ACM Symposium on User Interface Software and Technology* (Virtual Event, USA) (*UIST '21*). Association for Computing Machinery, New York, NY, USA, 985–996. doi:10.1145/3472749.3474800
- [51] Shan-Yuan Teng, Aryan Gupta, and Pedro Lopes. 2024. Haptic Permeability: Adding Holes to Tactile Devices Improves Dexterity. In *Proceedings of the 2024 CHI Conference on Human Factors in Computing Systems* (Honolulu, HI, USA) (*CHI '24*). Association for Computing Machinery, New York, NY, USA, Article 417, 12 pages. doi:10.1145/3613904.3642156
- [52] Hsin-Ruey Tsai, Chieh Tsai, Yu-So Liao, Yi-Ting Chiang, and Zhong-Yi Zhang. 2022. FingerX: Rendering Haptic Shapes of Virtual Objects Augmented by Real Objects using Extendable and Withdrawable Supports on Fingers. In *Proceedings of the 2022 CHI Conference on Human Factors in Computing Systems* (New Orleans, LA, USA) (*CHI '22*). Association for Computing Machinery, New York, NY, USA, Article 430, 14 pages. doi:10.1145/3491102.3517489
- [53] Nicha Vanichvoranun, Hojeong Lee, Seoyeon Kim, and Sang Ho Yoon. 2024. EStatiG: Wearable Haptic Feedback with Multi-Phalanx Electrostatic Brake for Enhanced Object Perception in VR. *Proc. ACM Interact. Mob. Wearable Ubiquitous Technol.* 8, 3, Article 131 (Sept. 2024), 29 pages. doi:10.1145/3678567
- [54] Michael White, James Gain, Ulysse Vimont, and Daniel Lochner. 2019. The Case for Haptic Props: Shape, Weight and Vibro-tactile Feedback. In *Proceedings of the 12th ACM SIGGRAPH Conference on Motion, Interaction and Games* (Newcastle upon Tyne, United Kingdom) (*MIG '19*). Association for Computing Machinery, New York, NY, USA, Article 7, 10 pages. doi:10.1145/3359566.3360058
- [55] Anusha Withana, Daniel Groeger, and Jürgen Steimle. 2018. Tacttoo: A Thin and Feel-Through Tattoo for On-Skin Tactile Output. In *Proceedings of the 31st Annual ACM Symposium on User Interface Software and Technology* (Berlin, Germany) (*UIST '18*). Association for Computing Machinery, New York, NY, USA, 365–378. doi:10.1145/3242587.3242645
- [56] Yunxiu XU, Siyu Wang, and Shoichi Hasegawa. 2024. Preserving Real-World Finger Dexterity Using a Lightweight Fingertip Haptic Device for Virtual Dexterous Manipulation. arXiv:2406.16835 [cs.HC] https://arxiv.org/abs/2406.16835

- [57] Andre Zenner and Antonio Kruger. 2017. Shifty: A Weight-Shifting Dynamic Passive Haptic Proxy to Enhance Object Perception in Virtual Reality. *IEEE Transactions on Visualization and Computer Graphics* 23, 4 (April 2017), 1285–1294. doi:10.1109/TVCG.2017.2656978
- [58] Yiwei Zhao and Sean Follmer. 2018. A Functional Optimization Based Approach for Continuous 3D Retargeted Touch of Arbitrary, Complex Boundariesnbsp;innbsp;Hapticnbsp;Virtual Reality. In *Proceedings of the 2018 CHI Conference on Human Factors in Computing Systems* (Montreal QC, Canada) (*CHI '18*). Association for Computing Machinery, New York, NY, USA, 1–12. doi:10.1145/3173574.3174118